Cell. Mol. Life Sci. (2011) 68:3233–3247
DOI 10.1007/s00018-011-0630-9

Cellular and Molecular Life Sciences

RESEARCH ARTICLE

Stimulation of olfactory ensheathing cell motility enhances olfactory axon growth

Louisa C. E. Windus · Fatemeh Chehrehasa · Katie E. Lineburg · Christina Claxton · Alan Mackay-Sim · Brian Key · James A. St John

Received: 18 November 2010 / Revised: 6 January 2011 / Accepted: 13 January 2011 / Published online: 12 February 2011

Abstract Axons of primary olfactory neurons are intimately associated with olfactory ensheathing cells (OECs) from the olfactory epithelium until the final targeting of axons within the olfactory bulb. However, little is understood about the nature and role of interactions between OECs and axons during development of the olfactory nerve pathway. We have used high resolution time-lapse microscopy to examine the growth and interactions of olfactory axons and OECs in vitro. Transgenic mice expressing fluorescent reporters in primary olfactory axons (OMP-ZsGreen) and ensheathing cells (S100ß-DsRed) enabled us to selectively analyse these cell types in explants of olfactory epithelium. We reveal here that rather than providing only a permissive substrate for axon growth, OECs play an active role in modulating the growth of pioneer olfactory axons. We show that the interactions between OECs and axons were dependent on lamellipodial waves on the shaft of OEC processes. The motility of OECs was mediated by GDNF, which stimulated cell migration and increased the apparent motility of the axons, whereas loss of OECs via laser ablation of the cells inhibited olfactory axon outgrowth. These results demonstrate that the migration of OECs strongly regulates the motility of axons and that stimulation of OEC motility enhances axon extension and growth cone activity.

L. C. E. Windus · F. Chehrehasa · K. E. Lineburg · A. Mackay-Sim · J. A. St John (✉)
National Centre for Adult Stem Cell Research, Eskitis Institute For Cell and Molecular Therapies, Griffith University, Nathan 4111, Brisbane, QLD, Australia
e-mail: j.stjohn@griffith.edu.au

L. C. E. Windus · C. Claxton · B. Key
School of Biomedical Sciences, University of Queensland, Brisbane, QLD, Australia

Keywords Neuron · OEC · GDNF · Lamellipodia · Glia · ZsGreen

Introduction

One of the unique characteristics of the mammalian olfactory system is that primary olfactory neurons turnover throughout life and rapidly regenerate after injury or disease. During development and in the adult, the newly formed axons extend from the neuroepithelium lining the nasal cavity along the olfactory nerve in the peripheral nervous system (PNS) and enter the nerve fibre layer of the olfactory bulb within the central nervous system (CNS) [1]. Thus, primary olfactory neurons not only continuously regenerate throughout life, but their axons also cross the PNS-CNS boundary.

Olfactory ensheathing cells (OECs) are the glia of the primary olfactory system and are intimately associated with primary olfactory axons along the length of their trajectory. OECs have some properties that are similar to both Schwann cells and astrocytes [2], but OECs are unique amongst the glia as they populate the olfactory nerve within both the PNS and CNS [1, 3]. While it is known that OECs express a range of molecules that promote olfactory axon adhesion, growth and guidance [1, 4–10], we know little of how, at the cellular level, OECs and primary olfactory axons interact to coordinate axon growth and guidance.

During development [11] as well as regeneration [12] OECs migrate ahead of primary olfactory axons. In contrast, Schwann cells migrate along already defined axonal pathways during development of the peripheral nervous system [13]. It is only during regeneration that Schwann cells, like OECs, migrate ahead of regrowing peripheral

axons [14]. In assays using olfactory epithelial explants in vitro, we have also demonstrated that OECs establish the field over which olfactory axons extend and that, as in vivo, OECs always migrate ahead of axons [12]. Thus, it would appear that both in vivo and in vitro, the growth and guidance of olfactory axons are tightly associated with the growth and guidance of OECs. We have previously reported that lamellipodial waves along the shaft of the OEC processes regulate interactions between OECs and that stimulation of the lamellipodial activity by GDNF increases cell-cell contact and migration of OECs [15, 16]. However, it remains unclear how the activity of OECs can influence the growth and motility of olfactory axons and whether the lamellipodial waves play a role in axon-to-OEC contact.

OECs have been trialled for neural regeneration therapies with several studies demonstrating improved axon regeneration although with varying success [17–19]. In some models of spinal injury transplants, OECs have migrated substantial distances into the injured spinal cord [20–22] perhaps due to their attraction to reactive astrocytes [23]. In other spinal injury models, migration of OECs has been limited [24, 25]. In other regions of the nervous system, explanted OECs can migrate along the optic nerve and ensheathe retinal ganglion cell axons [26], and they can also restore sensory input in brachial plexus injuries [27]. Recently it has been shown that diffusible factors, extracellular matrix factors and membrane-bound factors expressed by OECs have distinctly different effects on neurogenesis in cultured neural stem cells [28]. It is now clear that if the role of OECs in facilitating axon growth were better understood, then more effective therapies in humans could be developed.

To begin to address the role of OECs in olfactory axon growth, we have used high resolution time-lapse microscopy in transgenic reporter mice expressing bright fluorescent proteins in olfactory axons and OECs. We report here that lamellipodial waves on OECs are the point of contact for axons and that the migration of OECs directly influences olfactory axon motility and migration. These results have important implications for the use of OECs in neural regeneration therapies.

Materials and methods

Fixed tissue analysis

Postnatal OMP-ZsGreen mice [16] and embryonic OMP-ZsGreen mice crossed with S100ß-DsRed mice [15] were decapitated and heads were fixed in 4% paraformaldehyde at 4°C, cryoprotected in 30% sucrose with 0.1% sodium azide and then placed in embedding matrix (O.C.T. compound, Miles Scientific, Naperville, IL, USA) and snap frozen by immersion in iso-pentane that had been cooled by liquid nitrogen. Serial coronal sections (30 µm) were cut on a cryostat microtome, mounted on glass slides and then coverslipped with anti-fade mounting medium. All procedures were carried out with the approval of, and in accordance with, the Griffith University Animal Ethics Committee, the University of Queensland Animal Ethics Experimentation Committee and the Australian Commonwealth Office of the Gene Technology Regulator.

Preparation of olfactory epithelium explant culture

Timed pregnant OMP-ZsGreen transgenic mice or OMP-ZsGreen × S100ß-DsRed [15, 16] transgenic mice were killed by 5% CO_2 gas asphyxiation and E11.5–E14.5 embryos were decapitated. Olfactory epithelium was dissected from the nasal septum and the underlying lamina propria was removed using superfine forceps. Explants were plated on Matrigel basement membrane matrix (BD Bioscience, 1:10) coated on glass bottom cell culture dishes. The explants were cultured in complete medium (CM) containing Neurobasal medium (Gibco Invitrogen) supplemented with 0.4% methyl cellulose (BDH Chemical), 1× B27 serum-free supplement (Gibco Invitrogen), 0.8 mM L-glutamine (Gibco Invitrogen), 10 mM HEPES and 5 µg/ml gentamycin (Gibco Invitrogen) at 37°C and 5% CO_2. Robust axon outgrowth was evident after 24 h in culture.

Dissociated cultures of OECs and olfactory neurons

Olfactory epithelium was dissected from OMP-ZsGreen × S100ß-DsRed transgenic mice as described above. Explants were then treated in Dispase for 5 min in a water bath at 37°C, washed with Hanks balanced salt solution (HBSS), triturated and then plated onto Matrigel basement membrane matrix (1:10) coated on 96-well glass bottom cell culture plates. Dissociated tissue was maintained in CM at 37°C and 5% CO_2.

Growth factor and inhibitor assays of OE explants

Olfactory epithelium (OE) from E11.5–E14.5 OMP-ZsGreen × S100ß-DsRed transgenic embryos were grown for 24 h. OE explants were imaged 20 min prior to the incubation, and then each of the following were added to the culture medium: recombinant human glial cell line-derived neurotrophic factor (GDNF, Bio-Scientific, NSW, Australia), nerve growth factor (NGF, Invitrogen, Melbourne, Australia) at final concentrations of 10 and 20 ng/ml, JNK inhibitor II SP600125 (50 nM, Sigma-Aldrich), Src family kinase inhibitor PP2 (5 µM; Calbiochem, Merck, Darmstadt,

Germany) and the inactive analogue PP3 (5 μM; Calbiochem). Images were then taken at 20 and 40 min post incubation.

Live cell and fixed tissue imaging

Time-lapse images were routinely collected at intervals of 2–5 min over periods of 2–3 h using an AxioCam MRm digital camera and a Uniblitz VCM01 shutter on an inverted Zeiss Axioobserver Z1 microscope fitted with epifluorescence and differential interference contrast optics. Images were collected with a Zeiss LD PlanNeo-FLUAR 25/0.8 water iris, a LD PlanNeo-FLUAR 20/0.75 air iris and a LD PlanNeo-FLUAR 60/1.1 oil iris. During imaging culture plates were maintained at 37°C in an incubator chamber with 5% CO_2. Images were compiled using Axiovision Rel 4.6.3 (Zeiss, Germany) and colour-balanced in Adobe Photoshop v. 10.0 without further digital manipulation. Images of fixed tissue were collected on an Olympus BX50 microscope fitted with fluorescence optics and captured using a Spot camera and software, or with an Olympus FV-1000 confocal microscope.

Laser ablation assay

OE explants from E11.5–E14.5 OMP-ZsGreen × S100ß-DsRed transgenic embryos were cultured as described above. Regions of explants that clearly displayed OEC and axon outgrowth onto the matrix were chosen using an Olympus FV-1000 scanning confocal microscope. Using the laser bleach function of the Olympus Fluoview ver. 1.7b software (Olympus, Tokyo), cell bodies of OECs within a small region external to the explant were individually exposed. Each cell received 10–15 min of DsRed fluorophore specific laser ablation. The complete medium was changed directly after the ablation procedure to remove associated apoptotic cell toxins from the culture. Post ablation images were collected at 2 and 8 h. Controls consisted of regions of the same explants where OECs were not ablated.

Quantification of OEC migration rates and determination of axon length

Time-lapse image sequences of primary olfactory axons and OEC cultures were collected and analysed with Imaris analysis software (Bitplane Scientific Solutions). The Dots Tracer function of the Imaris analysis software was used to trace the migration rate of OECs which calculated the total distance travelled by the cell body over the total recording period. Total primary olfactory axon length from olfactory epithelium explants was determined using the Filament Tracer function of the Imaris analysis software. Total distance between axon shafts was obtained from the Filament Tracer function for axons and the Dots Tracer function for OECs. To analyse the effects of growth factor and inhibitor assays, we compared mean percentages of given measures from the same explant prior to and after the addition of factors. Statistical analysis was carried out using Graph-Pad Prism (version 4), and statistical significance for all given variables was tested using a Kruskal-Wallis test and Dunn's multiple comparison test for post hoc analysis.

Results

Pioneer olfactory axons actively grow in vitro

In order to determine the cellular interactions that occur during primary olfactory axon and OEC migration, we utilised two transgenic lines of mice: OMP-ZsGreen transgenic mice [16] and S100ß-DsRed transgenic mice [15]. In the OMP-ZsGreen mice, the cell bodies of primary olfactory neurons in the olfactory epithelium as well as their axons that terminate in glomeruli in the olfactory bulb express the very bright and stable ZsGreen protein (Fig. 1a). In explants of olfactory epithelium obtained from embryonic day 12.5 (E12.5) OMP-ZsGreen mice, the neuronal bodies within the explant tissue were clearly evident (Fig. 1b, arrowheads) which enabled us to detect nascent axons extending out of the explant within 5 h of plating (Fig. 1b, arrow). After 24 h in culture, olfactory receptor neuron axons extensively grew out from the explant in fasciculated bundles (Fig. 1c, arrow), reminiscent of the behaviour of axons in vivo. As previously described, OECs express DsRed protein in the S100ß-DsRed transgenic mouse line [15]. A cross-sectional view of an axon fascicle from a cross between OMP-ZsGreen and S100β-DsRed mice revealed the intimate association of axons with OECs, with the processes of the OECs not only surrounding the fascicles (arrow in Fig. 1d–f) but also forming conduits within the fascicles through which the axons travelled (arrowhead in Fig. 1d–f).

We used time-lapse microscopy over 1–2 h periods to begin to understand the behaviour of axons as they extended away from the explants. As reported for other axons [29–31], olfactory axons displayed intermittent periods of high growth activity marked by dynamic exploration of the local environment by growth cones (Fig. 1g). Active growth cones extended broad membranous sheets of lamellipodia and finer spike-like filopodial processes (Fig. 1g, 43.07, arrow). Axons also displayed periods of inactivity marked by retraction of the lamellipodia and simple bullet-shaped morphologies (Fig. 1g, 10.49, arrow). Pioneer axons were present at the outermost

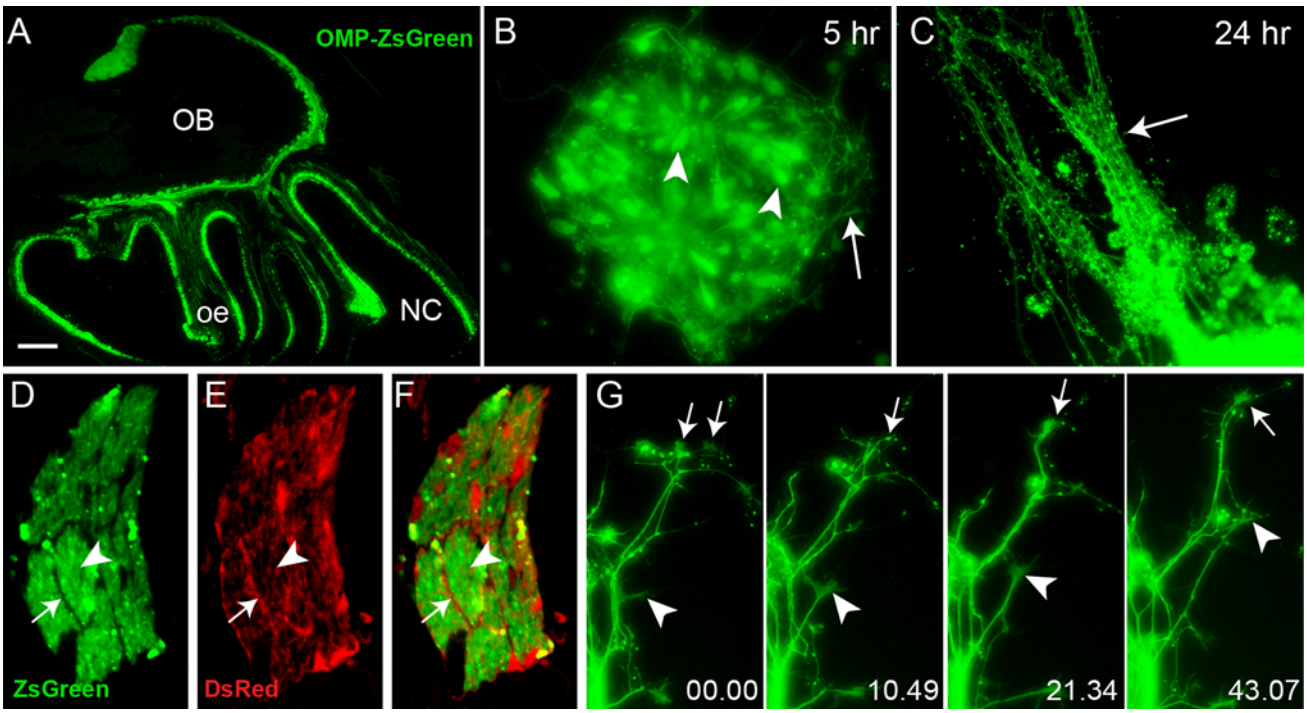

Fig. 1a–g Olfactory sensory axons extend rapidly in vitro. **a** P2.5 sagittal section of an OMP-ZsGreen transgenic mouse. Primary olfactory axons express the bright fluorescent protein ZsGreen. **b** An olfactory epithelium explant prepared from an E12.5 OMP-ZsGreen embryo. After 5 h in culture primary olfactory neurons (*arrowheads*) were clearly evident and extended nascent axons over the surface of the culture dish (*arrow*). **c** After 24 h, axons extended out of the explant and formed tightly fasciculated bundles (*arrow*). **d–f** High magnification view of a cross section through an olfactory sensory axon fascicle; axons (ZsGreen) are ensheathed by olfactory ensheathing cells (DsRed). The OECs line the perimeter (*arrow*) of fascicles within the large nerve bundle; fine processes (*arrowhead*) of OECs were also within the fascicle. **g** Panels show high magnification time-lapse microscopy of ZsGreen-positive axons in culture. Two pioneer axons with active growth cones (*arrows* 0.00) interacted with each other (*arrow* 10.49) and fasciculated together (*arrow* 21.34–43.07) whilst continuing to extend out from the explant. A follower axon extended along the length of the pre-existing axons (*arrowhead* 0.00). As it extended its active growth cone (*arrowhead* 10.49), it directly followed and remained in contact with the pre-existing axons (*arrowhead* 10.49–43.07) via the extension of thin filopodia. Time is recorded in minutes and seconds. *OB* Olfactory bulb, *NC* nasal cavity, *oe* olfactory epithelium. *Scale bar* 900 μm in **a**, 10 μm in **b**, 40 μm in **c**, 7 μm in **d–f**, 20 μm in **g**

peripheral margin of explants (Fig. 1g, 00.00, arrows). It was often observed that several pioneer axons extended out along separate trajectories (Fig. 1g, 00.00, arrows) and then interacted and fasciculated with each other (Fig. 1g, 10.49–43.07, arrows). Secondary or follower axons (Fig. 1g, arrowhead) were seen to extend directly along the pre-existing scaffold laid down by pioneer axons, and the growth cones actively anchored themselves to the pioneer axons (Fig. 1g, 10.49–43.07, arrowhead). These results are consistent with the development of axon scaffolds in vivo [32–34].

OECs regulate pioneer olfactory axon motility

Previous studies have revealed that both dorsal root ganglion and retinal ganglion cell axons avidly extend directly across a substrate of extracellular matrix in vitro [29, 30], whereas olfactory axons appear to instead avoid growing on this substrate and preferentially grow on OECs [9]. In order to determine how OECs influence axon growth, we used time-lapse and a combination of differential inference contrast optics (DIC) with fluorescence imaging to better characterise the behaviour of olfactory axons as they grew out from explants while in contact with OECs. Olfactory epithelium explants derived from the OMP-ZsGreen and S100ß-DsRed transgenic crosses provided clear identification of both OECs (Fig. 2a–c, arrows) and olfactory axons (Fig. 2a, unfilled arrowheads) in culture. The OECs appeared to form chains of cells as they migrated away from the explant (Fig. 2a–c, arrows). While small numbers of non-DsRed-positive cells also migrated out of the explants, olfactory axons were never associated with them (Fig. 2c, arrow with tail). Olfactory axons (Fig. 2a, unfilled arrowheads) clearly only extended across the surface of DsRed-positive OECs. Consistent with previous findings [9, 11, 12], OECs were found to lead the pioneer axons present at the outer most peripheral regions (Fig. 2a, arrow). This intimate relationship between OECs and olfactory axons was further examined in dissociated cultures. Olfactory neurons that were not in direct cell-cell

contact with an OEC rarely extended an axon (5%; $n = 40$) despite being in close proximity to OECs. In contrast, neurons that were in contact with an OEC showed rigorous axon outgrowth (Fig. 2d). While the filopodia of the growth cones sampled the extracellular matrix (arrowhead, Fig. 2d) the growth cones themselves only progressed forwards when in direct contact with an OEC, and then only along the shaft of an OEC (Fig. 2e, arrow). The axons maintained close contact with the cell body and lamellipodial waves that emanated from the shaft of the OECs (Fig. 2e, asterisk) and then continued elongating by growing from the shaft of one OEC to the next within a chain (Fig. 2e, unfilled arrowhead). These results suggest that olfactory axon outgrowth and extension in vitro are predominantly dependent upon direct cell-cell contact with OECs and that soluble factors released by OECs are insufficient for initial axon extension.

Lamellipodial waves mediate contact between olfactory axons and OECs

We have previously shown that motile lamellipodial protrusions, termed lamellipodial waves, are present on the shafts of peripherally derived OECs and are crucial for mediating cell-cell contact and migration [15]. We therefore investigated whether lamellipodial waves were involved in mediating cell-cell contact between olfactory axons and OECs. Using high resolution time-lapse microscopy we analysed cell interactions in olfactory epithelium explant cultures derived from OMP-ZsGreen × S100ß-DsRed mice. The dynamic peripheral lamellipodia were present along the shaft of OECs (Fig. 2f, 00.00, unfilled arrowhead) and were distinct from the leading edge (Fig. 2f, 00.00, arrow with tail). We consistently found that the growth cone of an olfactory axon initiated a cell-cell interaction with an OEC via contact with an active lamellipodial wave (Fig. 2g, filled arrowhead) and that lamellipodial waves were nearly always present at the site of initial contact between axons and OECs (92%; $n = 32$). Thus, an axon would only move from the shaft of one OEC to another when its growth cone interacted with a lamellipodial wave on the new OEC (Fig. 2f, g, arrowheads). The axon then remained adhered to this OEC process over the period of the recording (Fig. 2i, k, filled arrowheads). When the lamellipodial wave dynamically moved in an anterograde direction along the shaft of the OEC (Fig. 2h, 9.20, arrowhead) the growth cone of the axon extended a filopodia (Fig. 2i, arrow) and directly interacted with the lamellipodial wave. After interacting with the lamellipodial wave, the filopodia formed an additional axonal branch that remained adhered to the OEC process (Fig. 2k, arrow). These results suggest that lamellipodial waves are cellular processes that not only initiate cell-cell contact between axons and OECs, but are involved in promoting axon branch formation.

Axon motility mirrors OEC movement

We next examined the temporal nature of the interactions between OEC and pioneer olfactory axons. We found that OECs (Fig. 2l, 00.00, unfilled arrowhead) were consistently present at the leading edge of olfactory axons. Pioneer olfactory axons would clearly adhere along the length of the leading OEC (Fig. 2l, 00.00, arrow). The leading OEC migrated across the extracellular matrix substrate (Fig. 2l, 1.00.00, unfilled arrowhead) while the olfactory pioneer axon remained directly adhered to the cell (Fig. 2l, 1.00.00, arrow). Olfactory axons directly responded to the movement of OECs (Fig. 2l, 1.15.24, unfilled arrowhead) by actively exploring the shaft of the motile OEC with its growth cone and its numerous filopodia (Fig. 2l, 1.15.24, arrow). The olfactory axons (Fig. 2l, 1.30.57–1.46.32, arrows) appeared to respond to the change in morphology of the leading OEC (Fig. 2l, 1.30.57–1.46.32, unfilled arrowheads). These results suggest that olfactory axons not only preferentially grow over the surface of OECs, but their elongation is largely determined by the motility of OECs in culture. We further confirmed the dependence of axon motility on OEC migration using fluorescent time-lapse microscopy combined with DIC optics to better visualise the underlying OECs (Fig. 3). The olfactory axons adhered to and aligned themselves along the predominantly bipolar OECs (Fig. 3d–o). When the OECs migrated across the substrate (Fig. 3h–k), olfactory axon extension and movement directly mirrored the migratory pattern of the OECs (Fig. 3l–o). Moreover, while filopodia occasionally explored the surrounding area, the olfactory axons and their growth cones were never seen to actively extend beyond the cellular boundaries of the OECs. These results suggest that olfactory axon migration and pathfinding in vitro are dependent on the motility of migrating OECs.

GDNF regulates olfactory axon extension via OEC migration

We have previously reported that GDNF is an important regulator of OEC migration [15]. Addition of exogenous GDNF was shown to increase OEC migration while inhibition of GDNF-based signalling with selective inhibitors of either JNK (SP600125; [35]) or SRC (PP2; [36]) significantly decreased OEC migration [15]. We next tested whether GDNF also modulates changes in OEC migration in the presence of axons in vitro, and if so, whether OEC migration would in turn affect olfactory axon outgrowth. We examined the effect that exogenous GDNF had on

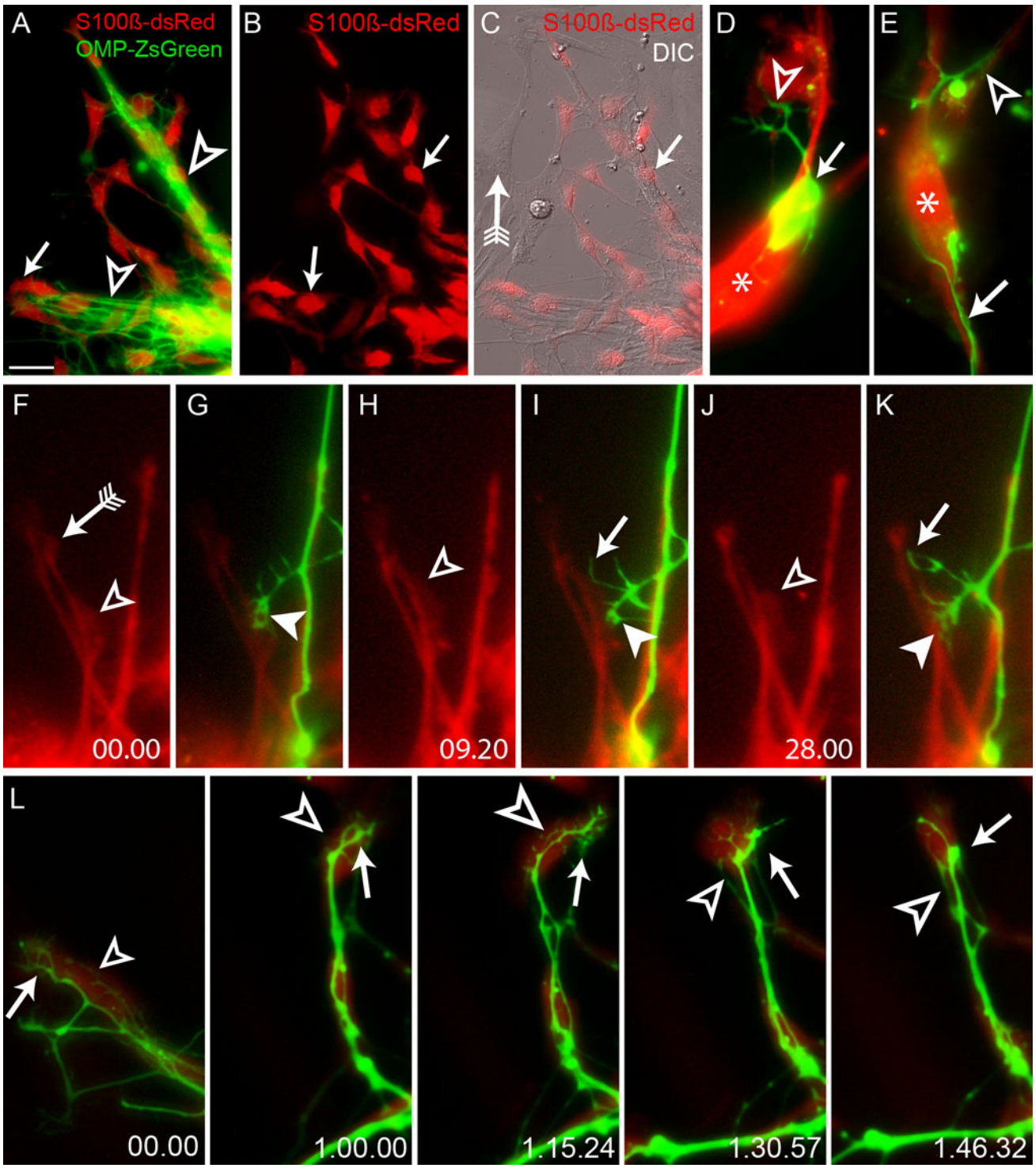

well-established olfactory epithelial explant cultures in which olfactory axons extended over a pre-existing scaffold of DsRed-positive OECs (Fig. 4b, unfilled arrowhead). We found that addition of exogenous GDNF (10–20 ng/ml) had a strong effect on the behaviour of both OECs and axons in comparison to control explants (Fig. 4a). In particular, the OECs migrated towards each other to form tightly adherent chains and the rate of OEC migration significantly increased. We measured the rate of migration of the OECs and we quantified the degree of cell-cell contact by measuring the distance between OECs. Addition of exogenous GDNF significantly increased the rate of

◀**Fig. 2a–l** Olfactory axon extension is limited by OECs. **a** A fluorescent ZsGreen image revealed that axons from an explant (out of view at *bottom right*) extended directly across a chain-like scaffold of OECs (*unfilled arrowheads*). OECs always migrated ahead of axons (*arrow*). **b** The fluorescent DsRed image revealed that OECs migrated out in a chain formation with OECs in direct contact with each other (*arrows*). **c** A merged DIC and fluorescent image of the same explant view revealed that DsRed-positive OECs (*arrow*) migrated out along with cells that were not DsRed-positive (*arrow with tail*), but that axons always were associated with OECs and not the other cells. **d** In dissociated cultures of ZsGreen neurons and DsRed OECs, a single neuron (*arrow*) adhered to the cell body of an OEC (*asterisk*) and extended a single axon which directly interacted with another OEC (*unfilled arrowhead*). **e** An olfactory axon directly adhered to and extended along the shaft of an OEC (*arrow*), wrapped around the cell body (*asterisk*) and then extended directly along the shaft of another OEC (*unfilled arrowhead*). **f–k** Time-lapse imaging revealed that olfactory axon growth cones (GC) formed adhesive contacts with OECs via lamellipodial waves. **f** OECs exhibited lamellipodial protrusions along their shafts (*unfilled arrowhead* 00.00) which were independent of the leading edge (*arrow with tail*). The GC (**g** *filled arrowhead*) of a follower axon directly interacted with the lamellipodial wave (**f** *unfilled arrowhead*). **h** After 9.20 min the lamellipodial wave moved along the shaft of the OEC in an anterograde direction (*unfilled arrowhead*). **i** A filopodia (*arrow*) extended from the GC and interacted with the motile lamellipodial wave while the GC remained adhered to the OEC process (*arrowhead*). **j** The lamellipodial wave remained active over the course of 28 min (*unfilled arrowhead*). **k** The GC (*filled arrowhead*) remained adhered to the OEC via the lamellipodial wave (**j** *unfilled arrowhead*) while the filopodium (*arrow*) continued to adhere to the OEC process. **l** Time-lapse microscopy revealed that the extension and motility of pioneer axons mirrored that of OECs. A pioneer axon (*arrow*) adhered to the shaft of an OEC (*unfilled arrowhead*). The OEC actively migrated to the right of the field of view (*unfilled arrowheads*, 00.00–1.15.24) while the axons (*arrows*) adhered to and responded to the underlying activity of the OEC. The OEC then changed direction (*unfilled arrowhead*, 1.30.57–1.46.32) and actively migrated while the axon followed (*arrows*, 1.30.57–1.46.32). Time is recorded in hours, minutes and seconds. *Scale bar* 40 μm in **a–c**, 10 μm in **d–e**, 30 μm in **f–k**, 5 μm in **l**

OEC migration (Fig. 4b, c, +20.00, +40.00, arrows; Fig. 5a) and significantly decreased the average distance between OECs (Fig. 4b, c, +20.00, +40.00, unfilled arrowheads; Fig. 5b) in comparison to controls. The GDNF-mediated migratory behaviour was consistent with our previous findings in which GDNF stimulated contact-mediated migration in monocultures of OECs [15]. The behaviour of the axons closely mirrored that of the OECs. As the OECs migrated more closely together, the axons appeared to form tight fascicles (Fig. 4b, +40.00 min, arrowhead). We quantified the resultant effect on the axon growth in these cultures and found that addition of exogenous GDNF (10–20 ng/ml) significantly increased the average length of axons (Fig. 4b, +20.00, +40.00, filled arrowheads; Fig. 5c) and their degree of fasciculation (Fig. 5d). During the GDNF-dependent changes in motility of OECs, it became evident that the axons remained adherent to the OECs and that their behaviour appeared to merely reflect the migration of OECs. The action of GDNF was selective since nerve growth factor (NGF), which is also expressed by OECs [7], did not stimulate OEC migration (Fig. 5a).

We next examined the effect of reducing endogenous GDNF-based signalling using inhibitors of either JNK (SP600125) or SRC (PP2). When added to the culture medium, these inhibitors decreased OEC migration (Figs. 4d, e, 5a). The inhibitors of either JNK (SP600125) or SRC (PP2) signalling pathways decreased the average length of axons (Fig. 4d, e, +20.00, +40.00, unfilled arrowheads; Fig. 5c), whereas incubation with the inactive analogue PP3 or NGF had no effect (Fig. 5c). Incubation with the inactive analogue PP3 also had no effect on OEC migration (Fig. 5a). Together these results indicate that GDNF can indirectly regulate axon extension via directly modulating OEC migration and behaviour.

We have previously shown that exogenous GDNF in monocultures of OECs increases the size of lamellipodia on OECs [15]. We therefore examined whether the lamellipodia were similarly affected in the explant cultures in which OECs and axons were growing together. We found that application of exogenous GDNF (10–20 ng/ml) significantly increased the surface area of lamellipodial waves along the shaft of OECs (Fig. 5e) as well as the area of lamellipodia present at the leading edge of the cells (Fig. 5e, f). The growth cones of the olfactory axons also dramatically increased in size in response to the addition of GDNF (Fig. 5g, h). Moreover, 92% ($n = 78$) of growth cones displayed an increase in surface area in response to the addition of GDNF (Fig. 5i) when in direct contact with either lamellipodia of the leading edge or lamellipodial waves on the shafts present on OECs (Fig. 5i–k). Thus, the response of the growth cones mirrored the response of the lamellipodia on OECs. While we cannot rule out a direct effect of GDNF on the axons, these results suggest that GDNF stimulated an increase in lamellipodia on OECs which in turn provided a favourable growth surface for the growth cones of the axons.

OEC ablation affects axon survival and migration

We have shown that olfactory axons not only preferentially grow in close association with OECs, but their migration in vitro is largely dependent on the motility of OECs. We were interested in further understanding whether axon outgrowth was dependent on contact-mediated interactions with OECs. To investigate this we laser ablated some of the OECs lying external to the olfactory epithelium explant and in close proximity to outgrowing axons. Prior to the ablation procedure, DsRed-positive OECs were clearly present and were migrating out onto the surface of the culture dish (Fig. 6a, d, unfilled

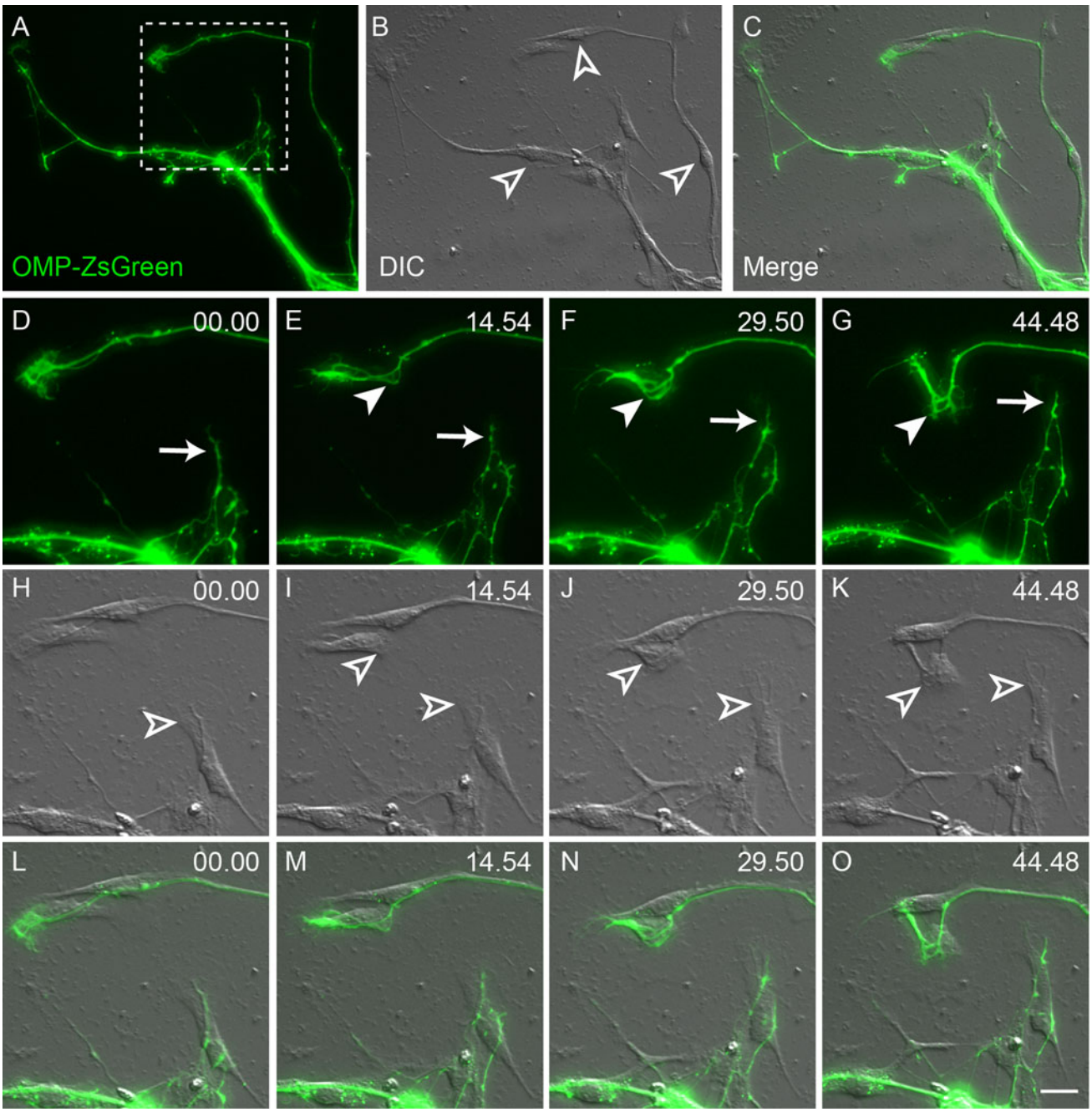

Fig. 3a–o The motility of olfactory axons is influenced by OEC migration. Panels show axons that have extended out of an E12.5 explant, imaged using ZsGreen fluorescence and differential inference contrast (DIC). **a** ZsGreen-positive axons extend from the explant which is out of view at the *bottom right*. **b** DIC imaging revealed the presence of numerous cells (*unfilled arrowheads*) underlying the axons. **c** Merged image of **a** and **b**. **d–o** Time-lapse imaging of the *boxed region* shown in **a**. **d–g** Some ZsGreen axons rapidly extended (*arrow*) during the imaging period, while others changed direction (*filled arrowhead*). **h–k** DIC imaging revealed that the underlying cells (*unfilled arrowheads*) migrated across the surface of the culture dish. **l–o** The ZsGreen-positive axons extended directly along the shaft and body of these cells. At no point did the axons extend out onto the matrix of the culture dish. Time is recorded in minutes and seconds. *Scale bar* is 15 μm in **a–c** and 3.5 μm in **d–o**

arrowheads) and within the explant tissue (Fig. 6d, black arrowhead). Olfactory axons (Fig. 6a, d, arrows) extended directly across the underlying OECs. During the ablation procedure, only OECs in a small region directly external to the explant tissue were treated while OECs in other areas around the explant were not ablated and therefore acted as an internal control. Two hours after the procedure, DsRed-positive OECs that were targeted for

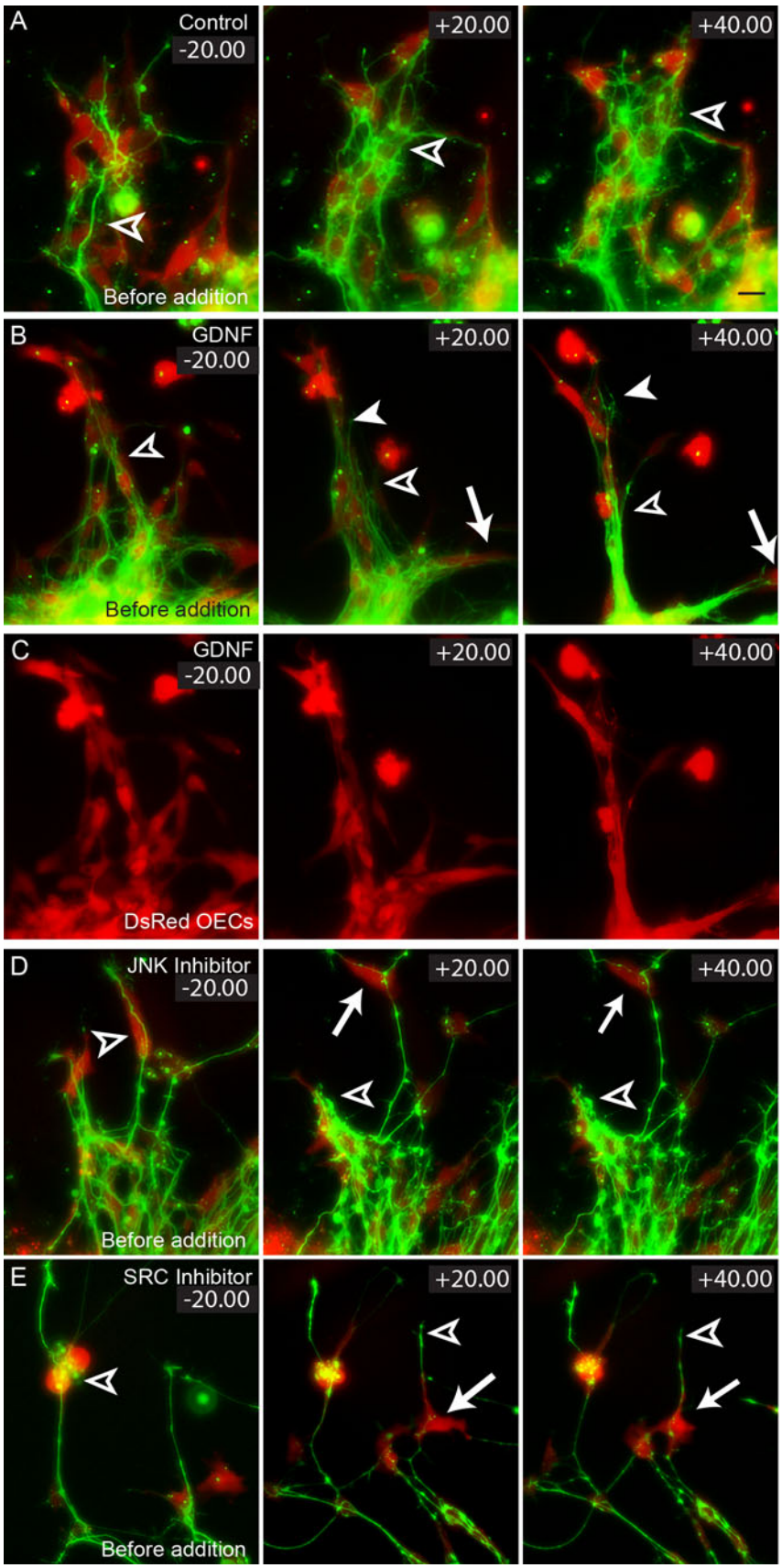

Fig. 4a–e The effect of GDNF on OECs and olfactory axon extension. Explants of olfactory epithelium were prepared from E14.5 OMP-ZsGreen × S100ß-DsRed embryos, cultured for 24 h and then incubated with either exogenous GDNF (**b**), JNK (**c**) or SRC inhibitors (**d**). **a–d** 20 min prior to challenging OE explants, olfactory axons extended along a chain-like scaffold of DsRed-positive OECs (*unfilled arrowheads*). **a** OECs (*red*) in control explants displayed limited migration and fasciculation during the imaging period. Extension of axons (*green*) was apparent only with follower axons (*unfilled arrowheads*). **b** After the addition of GDNF, OECs displayed higher migration rates (*arrows*, +20.00, +40.00) and formed tightly fasciculated bundles (*unfilled arrowheads*). Pioneer olfactory axons clearly exhibit additional extension and fasciculation (*filled arrowhead*). **c** DsRed-only fluorescence of images shown in **b** shows the changes in OEC distribution. **d** With the addition of JNK inhibitor, OEC migration (*arrows*, +20.00, +40.00) and axon extension (*unfilled arrowheads*) were minimal. **e** Similarly with the addition of SRC inhibitor, OEC migration (*arrows*, +20.00, +40.00) and axon extension (*unfilled arrowheads*) were minimal. Time is recorded in minutes and seconds. *Scale bar* 20 µm

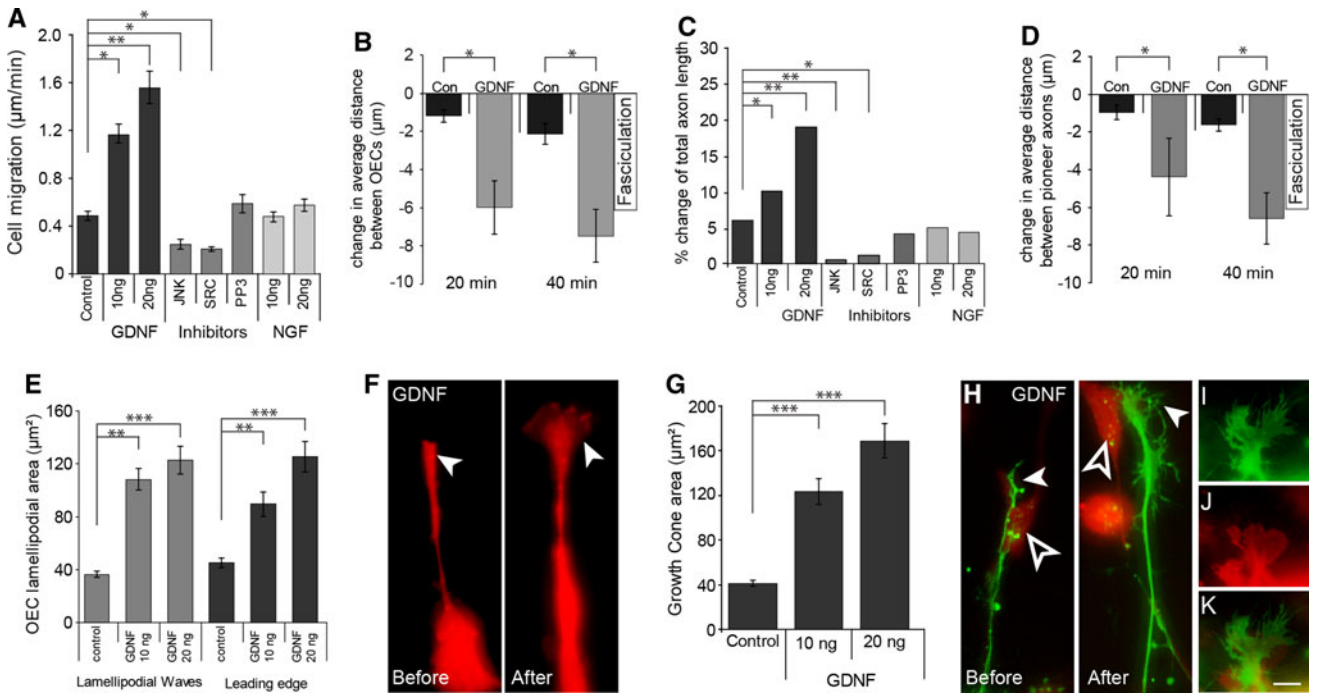

Fig. 5a–k GDNF influences OEC migration and pioneer axon extension. **a** OECs migrated at higher rates with addition of 10 and 20 ng/ml of GDNF; the addition of JNK (9SP600125) or SRC (PP2) inhibitors decreased migration of OECs; incubation with the inactive analogue PP3 or NGF had no effect on OEC migration ($n = 35$–40; $p < 0.01$, Kruskal-Wallis test and $^{*}p < 0.05$, $^{**}p < 0.01$, post hoc Dunn's multiple comparison test). **b** Quantification of the average distance between OECs when incubated with GDNF ($n = 10$; $p < 0.05$, Kruskal-Wallis test and $^{*}p < 0.05$, post hoc Dunn's multiple comparison test). **c** Quantification of pioneer axon extension. Axons extended at higher rates when incubated with 10 and 20 ng/ml of GDNF; the addition of JNK (9SP600125) or SRC (PP2) inhibitors decreased axon extension; incubation with the inactive analogue PP3 or NGF had no effect on axon extension ($n = 19$–20; $p < 0.01$, Kruskal-Wallis test and $^{*}p < 0.05$, $^{**}p < 0.01$, post hoc Dunn's multiple comparison test). **d** Quantification of the average distance between pioneer axons when incubated with GDNF ($n = 10$; $p < 0.05$, Kruskal-Wallis test and $^{*}p < 0.05$, post hoc Dunn's multiple comparison test. **e** Quantification of the surface area of lamellipodial waves and leading edge on OECs incubated with GDNF ($n = 40$–45; $p < 0.001$, Kruskal-Wallis test and $^{**}p < 0.01$, $^{***}p < 0.001$, post hoc Dunn's multiple comparison test). **f** Addition of GDNF dramatically increased the size of the leading edge on OECs. **g** Quantification of the surface area of growth cones (GC) on axons incubated with GDNF ($n = 38$–45; $p < 0.001$, Kruskal-Wallis test and $^{***}p < 0.001$, post hoc Dunn's multiple comparison test). **h** Addition of GDNF dramatically increased the size of the GC (*filled arrowhead*) on axons; example shown is one of the more dramatic increases in GC area. An underlying OEC (*unfilled arrowhead*) migrated during the assay. **i** There was a direct relationship between increased size in GC on axons and increased size of lamellipodia on OECs (**j**); GC size would increase when in direct contact with OEC lamellipodia (**k**). *Error bars* denote SEM. *Scale bar* 10 μm in **f**, **h**–**k**

ablation were no longer present beneath the axons (Fig. 6b, e; unfilled arrowheads). Only non-motile membrane fragments of OECs remained adherent to the surface of the culture dish after the treatment. Unablated DsRed-positive OECs remained active and viable both within the explant (Fig. 6b, black arrowheads) and in regions external to the explant that had not been targeted for ablation (Fig. 6h). In the OEC-ablated regions, although olfactory axons were clearly evident (Fig. 6b, e, arrows) their outgrowth had begun to decline 2 h after ablation of the OECs (Fig. 6i). Eight hours after the ablation there were clearly fewer olfactory axons (Fig. 6c, arrow) despite the presence of other non-DsRed cells migrating out from the explant (Fig. 6c; black arrowhead). In comparison, axons from the same explants growing over OECs that were not ablated continued to extend robustly over the same period (Fig. 6g–h). The average length of the axons in the OEC-ablated region significantly declined compared to axons in unablated control regions (Fig. 6i). After 8 h, olfactory axons had begun to extend from the explant (Fig. 6f, arrow) but always on the surface of underlying unablated DsRed-positive OECs (Fig. 6f, unfilled arrowhead). These results confirm that axon extension is reliant on an OEC scaffold in vitro.

Discussion

We have demonstrated here that OECs play an instructive role in olfactory axon growth. OECs are not only a preferential axonal substrate, but their motility regulates both

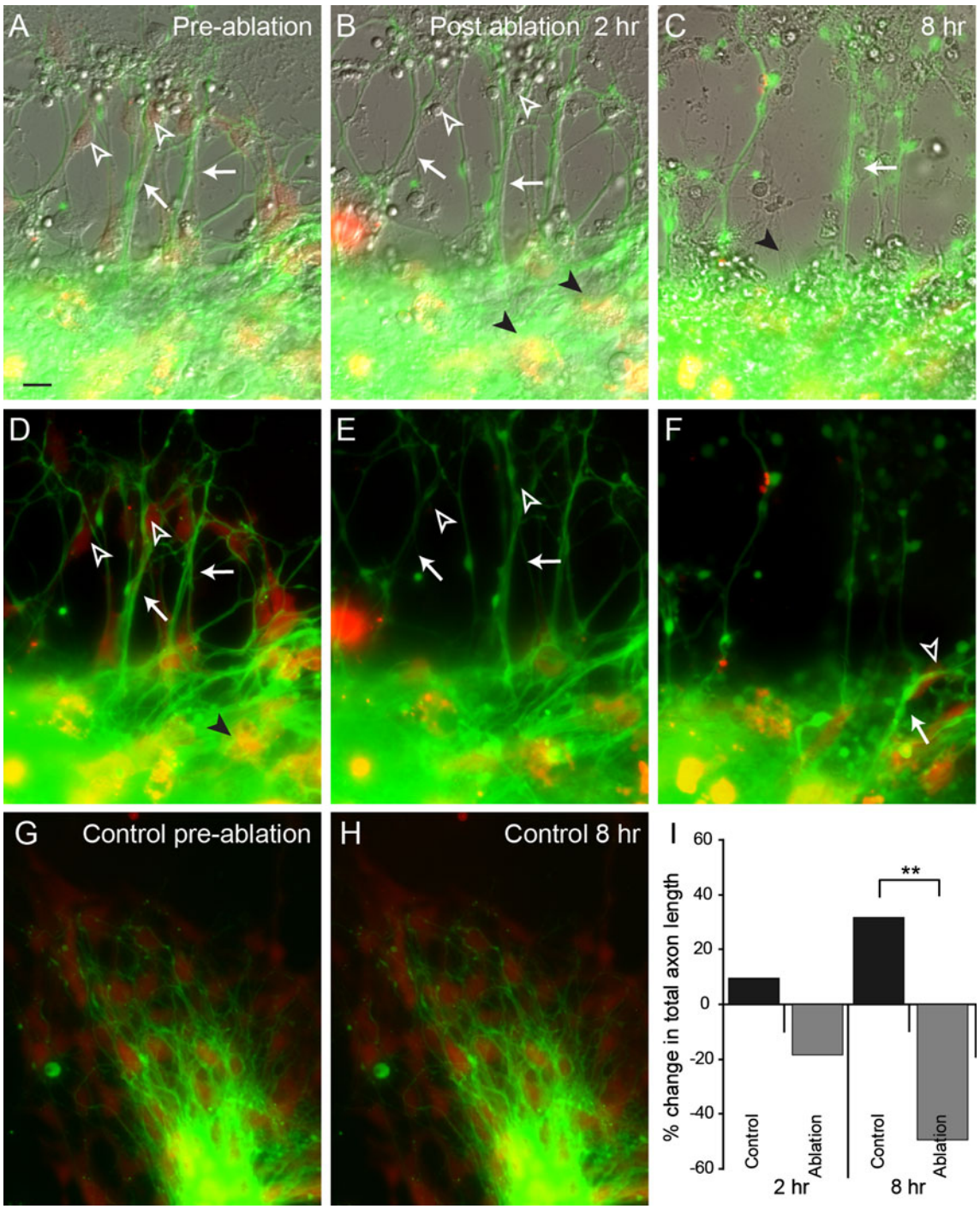

Fig. 6a–i Ablation of pre-existing OEC scaffolds inhibits olfactory axon extension. Panels **a–c** show fluorescence and DIC combined images; panels **d–f** show same images but without DIC. **a**, **d** Pre-ablation: DsRed-positive OECs migrated out of an explant onto the matrix forming a chain-like scaffold (*unfilled arrowheads*). ZsGreen-positive axons (*arrows*) extended directly across the OEC scaffold. **b**, **e** Two hours post ablation: DsRed-positive OECs were no longer present on the matrix (*unfilled arrowheads*) but remained active in the non-ablated region of the explant (*black arrowheads*). Olfactory axons remained active across the matrix (*arrows*). **c** Eight hours post ablation: very few olfactory axons remained within the ablated region (*arrow*) despite the presence of other cell types migrating across the matrix (*black arrowhead*). **f** DsRed-positive OECs started to migrate out of the explant (*unfilled arrowhead*) accompanied by the regrowth of olfactory axons (*arrow*). **g** For the control, a different region of the same explant was used. **h** OECs in the control region were not ablated and robust axon outgrowth occurred. *Scale bar* 20 μm in **a–f**; 40 μm in **g–h**. **i** Quantification of the change in axon length after ablating pre-existing OEC scaffolds. The length of olfactory axons significantly declined at 2 and 8 h post ablation compared to control axons grown on OECs of the same explants ($n = 7$; $p < 0.01$, Kruskal-Wallis test and $^{**}p < 0.01$, post hoc Dunn's multiple comparison test)

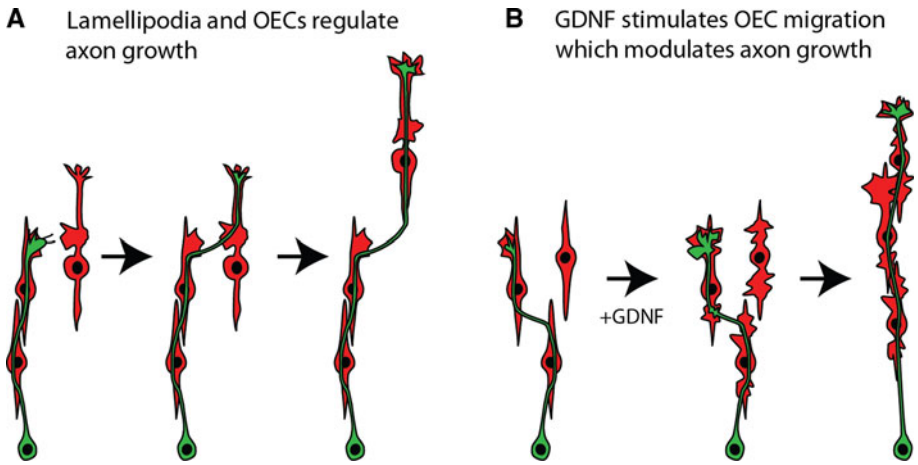

Fig. 7 **a** Olfactory axons (*green*) extend along the surface of OECs (*red*). Growth cones contact lamellipodial waves on OECs and then further extend along the new OEC. The migration of the OECs strongly regulates the motility of the axon. **b** GDNF stimulates the lamellipodial waves on OECs which results in close adhesion and contact-mediated migration of the OECs. The axons and their growth cones mirror the movement of the OECs

the elongation and guidance of olfactory axons. By modulating OEC migration with GDNF and inhibitors of the JNK and SRC kinases, we regulated the extent of olfactory axon elongation. We further revealed that the initial interactions between OECs and olfactory axons involved dynamic lamellipodial protrusions present along the shaft of OECs. Consistent with neuronal scaffold development studies [32, 33] our in vitro assays determined that initial pioneer olfactory axons serve as guides for later arising neurons and their processes. The olfactory axons clearly communicated with each other via their growth cones and fine filopodia that periodically appeared along the shaft of extending olfactory processes. These results mirror the behaviour of axons in vivo where every 30–90 days each regenerating olfactory axon [37, 38] follows the pathway created by the pre-existing axons. Our results highlight the intimate interactions between the OECs and olfactory axons during development and reveal OECs as the principal orchestrator leading the formation of the olfactory nerve pathway.

The key to the time-lapse studies was the use of the OMP-ZsGreen transgenic mouse in which the majority of primary olfactory neurons express the very bright and stable ZsGreen protein [16] that is several-fold brighter than GFP [39]. This protein is expressed along the length of the axons including the fine filopodia of the growth cones and enabled us to visualise the growth of olfactory axons in high detail using time-lapse imaging. When the OMP-ZsGreen mice were crossed with the S100ß-DsRed transgenic mice [15, 16], we were able to selectively visualise both OECs and olfactory axons during the same time-lapse sequence. When olfactory epithelium explant cultures were imaged using only green fluorescence, the growth of axons appeared to be highly dynamic. However, when imaged in combination with DIC optics or the red fluorescence channel to visualise DsRed-OECs, it was readily apparent that the motility of axons was closely linked to the migration of OECs. Using high resolution microscopy it became evident that the growth of olfactory axons in vitro was predominantly regulated by the motility of the underlying scaffold of OECs. Consistent with other studies [6, 40, 41], OECs clearly served as a substrate for axon elongation. However, previously published results that have examined axon growth in vitro have not always considered the role of OECs in regulating the growth of axons [42] and thus the interpretation of assays of axon growth may be more complicated when OECs are included.

The growth and guidance of retinal axons which make contact with oriented extracellular channels in the embryonic chick retina are regulated and directed by the close contact to glia [43]. Similarly, in our olfactory epithelium explant assays, olfactory axon extension and pathfinding were largely determined by, and limited by, the shape and extent of the underlying substrate of motile OECs. However, unlike hippocampal neurons whose axons can grow in the absence of glia [44, 45], pioneer olfactory axons were very rarely seen to actively move from one OEC to another and were never seen extending without OECs near the growth cone. Thus, these results clearly demonstrate that the outgrowth of olfactory axons in vitro is dependent on the underlying OEC motility. Consistent with these results, we have recently demonstrated in vivo that during widespread regeneration olfactory axon extension can be significantly increased if the OECs are given conditions that promote their migration [12].

We have previously reported that peripheral OECs exhibit highly dynamic lamellipodia along their shafts and are important mechanisms for initiating cell-cell interactions and mediating cell migration [15]. It has also been shown that isolated OECs in single cell assays can rapidly alter their morphology by producing large lamellipodia which subsequently alter migration rates of the OECs [46]. We have now shown that these highly motile plasma membrane protrusions are important in regulating OEC-axon cell interactions (Fig. 7a). Similar structures have been reported on other cells types including Schwann cells

[47] and fibroblasts [48] and have been implicated with myelinating peripheral axons and regulating the direction of migration, respectively. The fact that lamellipodial waves on OECs were nearly always present at the site of initial contact between OECs and axons suggests that lamellipodial waves may be a unique mechanism that mediates cross-talk and adhesion between the two cell types.

The OECs that migrated out of the olfactory epithelium explant often maintained close contact with each other and consequently the axons that extended out along the OECs formed loose fascicles. We have previously shown that GDNF increases the activity of lamellipodial waves which results in increased cell-cell contact and enhances contact-mediated migration of OECs [15]; and GDNF was demonstrated to increase OEC migration in a scratch assay [49]. In the olfactory epithelium explant assays, addition of GDNF dramatically increased adhesion of OECs to each other and increased their rate of migration. The resultant effect on olfactory axons was that they became more tightly fasciculated and elongated, however, it was evident that the behaviour of the axons was largely due to the movement of the underlying OECs (Fig. 7b). These results are consistent with previously reported findings in which the components of the extracellular matrix facilitate migration OECs resulting in increased neurite outgrowth [9]. Inhibition of JNK and SRC kinases reduces the activity of lamellipodial waves and stalls migration in monocultures of OECs [15]. The current olfactory epithelium explant results support those findings, and inhibition of the JNK and SRC kinases resulted in reduced axon lengths, likely as a result of the stalled migration of OECs. We cannot rule out that GDNF and the JNK and SRC inhibitors directly affected axon growth. GDNF is known to have positive effects on axon outgrowth and extension in other neuronal populations in culture [50–52]. However, our current results, together with our previously published results on the effect of GDNF on OECs [15], show that it was clear that OEC motility was dramatically affected by GDNF and that axons remained tightly adhered to OECs and mirrored the movement of the glia (Fig. 7b). GDNF dramatically affected the area of the lamellipodial waves and leading edge on the OECs, as well as increasing the area of the growth cones on the axons. However, again it appeared that the effect of GDNF on the axons was indirect as the expansion of the growth cone mirrored the expansion of the lamellipodia on the OECs. The increase in lamellipodial size on OECs was readily evident on isolated OECs which had no contact with axons consistent with our previous findings in OEC monocultures [15]. The expansion of the growth cones of axons, however, was always observed with a closely adhered OEC so it was not possible to determine whether the effect of GDNF directly affected the growth cones or indirectly affected them via the OEC. Nevertheless, the results are consistent with GDNF regulating lamellipodial activity on OECs which then stimulates growth cone activity in axons.

OECs have been reported to migrate slightly ahead of the primary olfactory axons en route to the olfactory bulb during development [11], and we have now shown that during widespread regeneration the OECs always lead the new axons [12]. In addition, the extent of olfactory axon regeneration can be significantly increased if the OECs are given prior opportunity to migrate ahead of the axons [12]. In contrast, dorsal root ganglion axons are able to regenerate but cannot successfully pass the CNS barrier which is due in part to the inability of Schwann cells to migrate within the CNS [53]. Thus, the unique ability of the primary olfactory system to constantly regenerate throughout life and to cross the PNS-CNS barrier is most likely due to the presence of the OECs rather than particular characteristics of primary olfactory axons. The ability of OECs to promote axon growth combined with their unique feature of being able to migrate from the PNS into the CNS has led to the investigation of OECs for neural regeneration therapies [54, 55]. By further understanding the biology of OECs, it may be possible to design improved strategies for the use of OECs for neural regeneration therapies. Together, our results demonstrate that OECs provide olfactory axons with a unique surface that involves contact-dependent signalling and that the migration of OECs strongly directs the motility of olfactory axons. Future work will identify the molecules that regulate contact-dependent adhesion of primary olfactory axons to OECs.

Acknowledgments This work was supported by a grant from the National Health and Medical Research Council to J.S. and B.K. (grant number 511006), funding to the National Centre for Adult Stem Cell Research from the Australian Government Department of Health and Aging (A.M.S.) and an Australian Postgraduate Award to L.W.

References

1. Doucette JR (1990) Glial influences on axonal growth in the primary olfactory system. Glia 3:433–449
2. Franceschini I, Barnett S (1996) Low-affinity NGF-receptor and E-N-CAM expression define two types of olfactory nerve ensheathing cells that share a common lineage. Dev Biol 173:327–343
3. Doucette JR (1989) Development of the nerve fiber layer in the olfactory bulb of mouse embryos. J Comp Neurol 285:514–527
4. Chuah MI, Choi-Lundberg D, Weston S, Vincent AJ, Chung RS, Vickers JC, West AK (2004) Olfactory ensheathing cells promote collateral axonal branching in the injured adult rat spinal cord. Exp Neurol 185:15–25
5. Chung RS, Woodhouse A, Fung S, Dickson TC, West AK, Vickers JC, Chuah MI (2004) Olfactory ensheathing cells promote neurite sprouting of injured axons in vitro by direct cellular contact and secretion of soluble factors. Cell Mol Life Sci 61:1238–1245

6. Kafitz KW, Greer CA (1999) Olfactory ensheathing cells promote neurite extension from embryonic olfactory receptor cells in vitro. Glia 25:99–110
7. Lipson AC, Widenfalk J, Lindqvist E, Ebendal T, Olson L (2003) Neurotrophic properties of olfactory ensheathing glia. Exp Neurol 180:167–171
8. St John JA, Key B (1999) Expression of galectin-1 in the olfactory nerve pathway of rat. Brain Res Dev Brain Res 117:171–178
9. Tisay KT, Key B (1999) The extracellular matrix modulates olfactory neurite outgrowth on ensheathing cells. J Neurosci 19:9890–9899
10. Woodhall E, West AK, Chuah MI (2001) Cultured olfactory ensheathing cells express nerve growth factor, brain-derived neurotrophic factor, glia cell line-derived neurotrophic factor and their receptors. Brain Res Mol Brain Res 88:203–213
11. Tennent R, Chuah MI (1996) Ultrastructural study of ensheathing cells in early development of olfactory axons. Brain Res Dev Brain Res 95:135–139
12. Chehrehasa F, Windus LC, Ekberg JA, Scott SE, Amaya D, Mackay-Sim A, St John JA (2010) Olfactory glia enhance neonatal axon regeneration. Mol Cell Neurosci 45:277–288
13. Jessen KR, Mirsky R (2005) The origin and development of glial cells in peripheral nerves. Nat Rev 6:671–682
14. Parrinello S, Napoli I, Ribeiro S, Digby PW, Fedorova M, Parkinson DB, Doddrell RD, Nakayama M, Adams RH, Lloyd AC (2010) EphB signaling directs peripheral nerve regeneration through Sox2-dependent Schwann cell sorting. Cell 143:145–155
15. Windus LC, Claxton C, Allen CL, Key B, St John JA (2007) Motile membrane protrusions regulate cell–cell adhesion and migration of olfactory ensheathing glia. Glia 55:1708–1719
16. Windus LC, Lineburg KE, Scott SE, Claxton C, Mackay-Sim A, Key B, St John JA (2010) Lamellipodia mediate the heterogeneity of central olfactory ensheathing cell interactions. Cell Mol Life Sci 67:1735–1750
17. Bartolomei JC, Greer CA (2000) Olfactory ensheathing cells: bridging the gap in spinal cord injury. Neurosurgery 47:1057–1069
18. Gudino-Cabrera G, Pastor AM, de la Cruz RR, Delgado-Garcia JM, Nieto-Sampedro M (2000) Limits to the capacity of transplants of olfactory glia to promote axonal regrowth in the CNS. Neuroreport 11:467–471
19. Ramer LM, Au E, Richter MW, Liu J, Tetzlaff W, Roskams AJ (2004) Peripheral olfactory ensheathing cells reduce scar and cavity formation and promote regeneration after spinal cord injury. J Comp Neurol 473:1–15
20. Boruch AV, Conners JJ, Pipitone M, Deadwyler G, Storer PD, Devries GH, Jones KJ (2001) Neurotrophic and migratory properties of an olfactory ensheathing cell line. Glia 33:225–229
21. Ramon-Cueto A, Nieto-Sampedro M (1994) Regeneration into the spinal cord of transected dorsal root axons is promoted by ensheathing glia transplants. Exp Neurol 127:232–244
22. Resnick DK, Cechvala CF, Yan Y, Witwer BP, Sun D, Zhang S (2003) Adult olfactory ensheathing cell transplantation for acute spinal cord injury. J Neurotrauma 20:279–285
23. Su Z, Yuan Y, Chen J, Cao L, Zhu Y, Gao L, Qiu Y, He C (2009) Reactive astrocytes in glial scar attract olfactory ensheathing cells migration by secreted TNF-alpha in spinal cord lesion of rat. PLoS One 4:e8141
24. Lakatos A, Barnett SC, Franklin RJ (2003) Olfactory ensheathing cells induce less host astrocyte response and chondroitin sulphate proteoglycan expression than Schwann cells following transplantation into adult CNS white matter. Exp Neurol 184:237–246
25. Ruitenberg MJ, Plant GW, Christensen CL, Blits B, Niclou SP, Harvey AR, Boer GJ, Verhaagen J (2002) Viral vector-mediated gene expression in olfactory ensheathing glia implants in the lesioned rat spinal cord. Gene Ther 9:135–146
26. Li Y, Li D, Khaw PT, Raisman G (2008) Transplanted olfactory ensheathing cells incorporated into the optic nerve head ensheathe retinal ganglion cell axons: possible relevance to glaucoma. Neurosci Lett 440:251–254
27. Ibrahim AG, Kirkwood PA, Raisman G, Li Y (2009) Restoration of hand function in a rat model of repair of brachial plexus injury. Brain 132:1268–1276
28. Cao L, Mu L, Qiu Y, Su Z, Zhu Y, Gao L, Yuan Y, Guo D, He C (2010) Diffusible, membrane-bound, and extracellular matrix factors from olfactory ensheathing cells have different effects on the self-renewing and differentiating properties of neural stem cells. Brain Res 1359:56–66
29. O'Connor TP, Duerr JS, Bentley D (1990) Pioneer growth cone steering decisions mediated by single filopodial contacts in situ. J Neurosci 10:3935–3946
30. Seeger M, Tear G, Ferres-Marco D, Goodman CS (1993) Mutations affecting growth cone guidance in *Drosophila*: genes necessary for guidance toward or away from the midline. Neuron 10:409–426
31. Tang J, Landmesser L, Rutishauser U (1992) Polysialic acid influences specific pathfinding by avian motoneurons. Neuron 8:1031–1044
32. Boyan G, Therianos S, Williams JL, Reichert H (1995) Axogenesis in the embryonic brain of the grasshopper *Schistocerca gregaria*: an identified cell analysis of early brain development. Development 121:75–86
33. Jacobs JR, Goodman CS (1989) Embryonic development of axon pathways in the *Drosophila* CNS. I. A glial scaffold appears before the first growth cones. J Neurosci 9:2402–2411
34. Jacobs JR, Goodman CS (1989) Embryonic development of axon pathways in the *Drosophila* CNS. II. Behavior of pioneer growth cones. J Neurosci 9:2412–2422
35. Bennett BL, Sasaki DT, Murray BW, O'Leary EC, Sakata ST, Xu W, Leisten JC, Motiwala A, Pierce S, Satoh Y, Bhagwat SS, Manning AM, Anderson DW (2001) SP600125, an anthrapyrazolone inhibitor of Jun N-terminal kinase. Proc Natl Acad Sci USA 98:13681–13686
36. Hanke JH, Gardner JP, Dow RL, Changelian PS, Brissette WH, Weringer EJ, Pollok BA, Connelly PA (1996) Discovery of a novel, potent, and Src family-selective tyrosine kinase inhibitor. Study of Lck- and FynT-dependent T cell activation. J Biol Chem 271:695–701
37. Mackay-Sim A, Kittel P (1991) Cell dynamics in the adult mouse olfactory epithelium: a quantitative autoradiographic study. J Neurosci 11:979–984
38. Mackay-Sim A, Kittel PW (1991) On the life span of olfactory receptor neurons. Eur J Neurosci 3:209–215
39. Wouters M, Smans K, Vanderwinden JM (2005) WZsGreen/+: a new green fluorescent protein knock-in mouse model for the study of KIT-expressing cells in gut and cerebellum. Physiol Genomics 22:412–421
40. Kafitz KW, Greer CA (1998) The influence of ensheathing cells on olfactory receptor cell neurite outgrowth in vitro. Ann NY Acad Sci 855:266–269
41. Sonigra RJ, Brighton PC, Jacoby J, Hall S, Wigley CB (1999) Adult rat olfactory nerve ensheathing cells are effective promoters of adult central nervous system neurite outgrowth in coculture. Glia 25:256–269
42. Treloar HB, Ray A, Dinglasan LA, Schachner M, Greer CA (2009) Tenascin-C is an inhibitory boundary molecule in the developing olfactory bulb. J Neurosci 29:9405–9416
43. Krayanek S, Goldberg S (1981) Oriented extracellular channels and axonal guidance in the embryonic chick retina. Dev Biol 84:41–50

44. Banker GA, Cowan WM (1977) Rat hippocampal neurons in dispersed cell culture. Brain Res 126:397–425
45. Kim SU (1973) Morphological development of neonatal mouse hippocampus cultured in vitro. Exp Neurol 41:150–162
46. Huang ZH, Wang Y, Cao L, Su ZD, Zhu YL, Chen YZ, Yuan XB, He C (2008) Migratory properties of cultured olfactory ensheathing cells by single-cell migration assay. Cell Res 18:479–490
47. Nodari A, Zambroni D, Quattrini A, Court FA, D'Urso A, Recchia A, Tybulewicz VL, Wrabetz L, Feltri ML (2007) Beta1 integrin activates Rac1 in Schwann cells to generate radial lamellae during axonal sorting and myelination. J Cell Biol 177:1063–1075
48. Pankov R, Endo Y, Even-Ram S, Araki M, Clark K, Cukierman E, Matsumoto K, Yamada KM (2005) A Rac switch regulates random versus directionally persistent cell migration. J Cell Biol 170:793–802
49. Cao L, Su Z, Zhou Q, Lv B, Liu X, Jiao L, Li Z, Zhu Y, Huang Z, Huang A, He C (2006) Glial cell line-derived neurotrophic factor promotes olfactory ensheathing cells migration. Glia 54:536–544
50. Pellitteri R, Russo A, Stanzani S (2006) Schwann cell: a source of neurotrophic activity on cortical glutamatergic neurons in culture. Brain Res 1069:139–144
51. Pellitteri R, Spatuzza M, Russo A, Stanzani S (2007) Olfactory ensheathing cells exert a trophic effect on the hypothalamic neurons in vitro. Neurosci Lett 417:24–29
52. Pellitteri R, Zicca A, Mancardi GL, Savio T, Cadoni A (2001) Schwann cell-derived factors support serotoninergic neuron survival and promote neurite outgrowth. Eur J Histochem 45: 367–376
53. Lankford KL, Sasaki M, Radtke C, Kocsis JD (2008) Olfactory ensheathing cells exhibit unique migratory, phagocytic, and myelinating properties in the X-irradiated spinal cord not shared by Schwann cells. Glia 56:1664–1678
54. Lindsay SL, Riddell JS, Barnett SC (2010) Olfactory mucosa for transplant-mediated repair: a complex tissue for a complex injury? Glia 58:125–134
55. Radtke C, Wewetzer K (2009) Translating basic research into clinical practice or what else do we have to learn about olfactory ensheathing cells? Neurosci Lett 456:133–136